ELSEVIER

International Journal of Mass Spectrometry 223–224 (2003) 639–646

International Journal of Mass Spectrometry

www.elsevier.com/locate/ijms

Calculated absolute cross section for the electron-impact ionisation of simple molecular ions

H. Deutsch [a], K. Becker [b,*], P. Defrance [c], U. Onthong [d], M. Probst [d], S. Matt [d], P. Scheier [d], T.D. Märk [d,e]

[a] *Institut für Physik, Ernst Moritz Arndt Universitat Greifswald, Domstr. 10a, D-17487 Greifswald, Germany*
[b] *Department of Physics, Stevens Institute of Technology, Hoboken, NJ 07030, USA*
[c] *Département de Physique, Université Catholique de Louvain, Chemin du Cyclotron, 2, B-1348 Louvain-la Neuve, Belgium*
[d] *Institut für Ionenphysik, Leopold Franzens Universität Innsbruck, Technikerstr. 25, A-6020 Innsbruck, Austria*
[e] *Department of Plasmaphysics, Univerzita Komenskeho, Mlynska dolina, 842 48 Bratislava 4, Slovak Republic*

Received 15 February 2002; accepted 13 June 2002

Abstract

We report the results of the application of the semi-classical Deutsch–Märk (DM) formalism to the calculation of the absolute electron-impact ionisation cross section of the molecular ions H_2^+, N_2^+, O_2^+, CD^+, CO^+, CO_2^+, H_3O^+/D_3O^+, and CD_4^+ for which experimental data have been reported. Where available, we also compare our calculated cross sections with calculated cross sections using the BEB method. The level of agreement between the experimentally determined and the calculated cross section is satisfactory only in a few cases. In most cases, the calculated cross sections exceed the measured cross sections, in some cases significantly, which is not surprising in view of the experimental complications in measuring ionisation cross sections of molecular ions due to the presence of competing channels for the formation of fragment ions such as dissociative excitation versus dissociative ionisation. (Int J Mass Spectrom 223–224 (2003) 639–646)

Keywords: Electron-impact ionisation; Cross section calculations; Molecular ions

1. Introduction

The Deutsch–Märk (DM) formalism [1,2] and the binary-encounter-Bethe (BEB) method of Kim and co-workers [3,4] are the two most widely used semi-rigorous methods to calculate absolute (total single) electron-impact ionisation cross sections for molecules. Both methods were originally developed for the calculation of atomic ionisation cross sections and were subsequently extended to neutral molecular targets. Recently, Kim et al. [5] extended their BEB method to molecular ions and calculated ionisation cross sections for the targets H_2^+, N_2^+, CO^+, and CD^+. Subsequently, Deutsch et al. [6] extended the DM formalism to the calculation of ionisation cross sections of molecular ions. The results of the DM calculations for the two molecular ions N_2^+ and CO_2^+ [6] were in satisfactory agreement with measured data [7,8] and in the case of N_2^+ also with the BEB calculation [5].

In this paper, we present a complete account of the application of the DM formalism to the calculation of

* Corresponding author. E-mail: kbecker@stevens-tech.edu

1387-3806/02/$ – see front matter
PII S1387-3806(02)00936-3

cross sections for the electron-impact ionisation of all molecular ions for which experimental data are available. These include the diatomic molecular ions H_2^+, N_2^+, O_2^+, CD^+ and CO^+ as well as the polyatomic molecular ions CO_2^+, H_3O^+/D_3O^+, and CD_4^+. The previously published calculations for N_2^+ and CO_2^+ [6] are also included here again and discussed briefly for reasons of completeness. In the case of CO_2^+ we also found it necessary to revise our previous analysis of the reported experimental data [8], which reduced level of agreement between experiment and calculation. We also compare our calculated cross sections with calculated cross sections based on the BEB method where available.

2. Background

The DM formalism was originally developed [9] for the calculation of atomic ionisation cross sections and has been modified and extended several times [1,2]. The DM formula expresses the atomic ionisation cross sections as the sum over all partial ionisation cross sections corresponding to the removal of a single electron from a given atomic sub-shell labelled by the quantum numbers n and l as

$$\sigma = \sum_{\mathrm{n,l}} g_{\mathrm{nl}} \pi (r_{\mathrm{nl}})^2 \xi_{\mathrm{nl}} \cdot f(U) \qquad (1)$$

where $(r_{\mathrm{nl}})^2$ is the square of the radius of maximum radial density of the (n,l) atomic sub-shell (column 1 in the tables of Desclaux [10]), ξ_{nl} refers to the number of atomic electrons in the (n,l) sub-shell, and the g_{nl} are appropriately chosen weighting factors which are given in [1]. The function $f(U)$ describes the energy dependence of the ionisation cross section where U is the reduced collision energy, $U = E/E_{\mathrm{nl}}$. E denotes the energy of the incident electron and E refers to the ionization energy in the (n,l) sub-shell (see [1,2] for details). The DM formula can be extended for the case of a molecular ionization cross section calculations provided one carries out a Mulliken or other molecular orbital population analysis [11,12] which expresses the molecular orbitals in terms of the atomic orbitals of the constituent atoms. Orbital population analyses can be obtained routinely for a large number of molecules and radicals using standard quantum chemistry codes, many of which are available in the public domain. These codes can also be used to obtain the necessary molecular structure information in cases where this information is not available otherwise. Essentially all quantum chemistry codes can also be applied to positively charged molecular ions.

In the present study, the orbital populations were derived from Hartree-Fock wave functions with the CEP-31* basis set [13] and the orbital energies were calculated via outer-valence Green's functions [14]. The function $f(U)$ in Eq. (1), which was also derived for neutral targets initially, can be applied to the case of molecular ions by replacing the neutral ionisation energy E_{nl} by the corresponding ionisation energy of the molecular ion. Thus all but one of the quantities in the DM formula in Eq. (1) can be extended to a molecular ion as a target in a straightforward fashion. The weighting factors g_{nl} which were derived semi-empirically from a fitting procedure using well-established ionisation cross sections of neutral atoms are the sole quantities that are inherently tied to neutral targets. In the present DM calculation the ionic character of the target is therefore only reflected in the population analysis of the molecular orbitals as a 'missing' electron which results in different populations ξ_{nl} and different energies E_{nl}. In essence, one might say that for instance the DM calculation for CO_2^+ treats the ion as an iso-electronic neutral BO_2 molecule with the orbitals of the CO_2^+ ion. A similar argument applies to the representation of the other ions. Our method in essence neglects the Coulomb interaction between the incident electron and the overall charge of the molecular ion. Plausibility arguments suggest that this is a valid approximation at high impact energies, but may fail at energies close to threshold.

3. Results and discussion

The electron impact induced ionisation of a molecular ion is a complex process which results in a variety

of reaction pathways. If one considers the triatomic molecular ion CO_2^+, electron-impact can lead to the formation of the doubly charged parent ion CO_2^{2+}

$$e^- + CO_2^+ \rightarrow CO_2^{2+} + 2e^- \quad (2a)$$

and to a variety of dissociative channels (dissociative ionisation, dissociative excitation) such as

$$e^- + CO_2^+ \rightarrow C^+ + O_2^+ + 2e^- \quad (2b)$$

$$e^- + CO_2^+ \rightarrow C^+ + O + O^+ + 2e^- \quad (2c)$$

$$e^- + CO_2^+ \rightarrow C^+ + O_2 + e^- \quad (2d)$$

$$e^- + CO_2^+ \rightarrow C^+ + O + O + e^- \quad (2e)$$

$$e^- + CO_2^+ \rightarrow O^+ + CO^+ + 2e^- \quad (2f)$$

$$e^- + CO_2^+ \rightarrow O^+ + CO + e^- \quad (2g)$$

$$e^- + CO_2^+ \rightarrow O^+ + C + O + e^- \quad (2h)$$

$$e^- + CO_2^+ \rightarrow O^+ + C + O^+ + 2e^- \quad (2i)$$

$$e^- + CO_2^+ \rightarrow CO^+ + O + e^- \quad (2j)$$

$$e^- + CO_2^+ \rightarrow C + O_2^{2+} + 2e^- \quad (2k)$$

$$e^- + CO_2^+ \rightarrow C + O^{2+} + O + 2e^- \quad (2l)$$

$$e^- + CO_2^+ \rightarrow C^{2+} + O_2 \text{ (or } 2O) + 2e^- \quad (2m)$$

Processes (2b), (2c), (2f), (2i), and (2k)–(2m) are dissociative ionisation channels, whereas the other processes reflect dissociative excitation channels. We note that dissociative ionisation channels that result in the formation of doubly charged fragment ions have in general comparatively small cross sections, which was also observed previously in ionisation and dissociative ionisation studies of the neutral CO_2 molecule [15–17].

It is obvious that the formation of a specific singly positively charged ion such as C^+ following electron impact on the molecular ion CO_2^+ can be the result of several competing processes (see (2b)–(2e) above), some of which, (2b) and (2c), are dissociative ionisation processes, whereas the others, (2d) and (2e), are dissociative excitation channels. While these processes can in principle not be distinguished from one another as long as only the C^+ ion is detected in an experiment, the ions produced in each of the four reactions (2b) through (2e) above have different appearance energies and different kinetic excess energy distributions, so that careful studies of the appearance energy and kinetic excess energy distribution of a given fragment ion often gives insight into the dominant formation process, at least to some extent. We note that the present DM calculations (as well as the BEB calculations of Kim et al. [5]) include only ionisation and dissociative ionisation processes, but not dissociative excitation. Thus, it is imperative for a meaningful comparison between experimental data and calculated cross sections to extract an estimate for the dissociative ionisation cross section from measured partial cross sections that include contributions from both dissociative excitation and dissociative ionisation.

3.1. The homonuclear diatomic ions H_2^+, N_2^+, and O_2^+

In the case of H_2^+(Fig. 1), we compare the results of the present DM calculation with the measured data of Peart and Dolder [18], with theoretical results

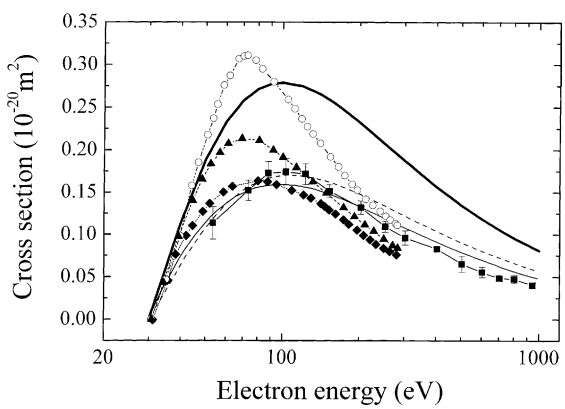

Fig. 1. Calculated absolute cross section for the electron-impact ionization of H_2^+ using the DM formalism as a function of electron energy (thick solid line) in comparison with the measured cross section of Peart and Dolder [18] (filled squares), two variants of the BEB method [5] (thin solid line and dashed line), a calculation by Alsmiller [20] (filled diamonds), and two calculations by Mathur et al. [19] using the classical impulse approximation (open circles and filled triangles).

[19,20] quoted in the paper of Peart and Dolder [18], and with the BEB calculation of Kim et al. [5]. There is good agreement between the experimental data and the calculations by Aismiller [20] and the two variants of the BEB calculation of Kim et al. [5] in terms of absolute cross section which reaches a maximum value of about 0.17×10^{-16} cm^2 at 100 eV as well as the cross section shape. The DM calculation results in a cross section maximum that is about 60% higher than these values, but describes the cross section shape quite well. We note that two variants of calculations by Mathur et al. [19] based on the classical impulse approximation yield cross section values that are closer to our calculation in terms of the maximum cross section value, but exhibit a different energy dependence.

The DM calculations for N_2^+ in comparison with the recent data reported by Defrance and co-workers [7], with earlier data reported by Peterson et al. [21] and with two calculated cross section curves using the BEB method with two different sets of ground-state wave functions for the target ion [5] were already discussed in our earlier letter [6]. The result is shown again here in Fig. 2. Peterson et al. [21] obtained their data by subtracting their measured cross section for dissociative excitation from the total cross section for N^+ production of Van Zyl and Dunn [22]. As a consequence, their data count the contribution to the cross section arising from symmetric dissociative ionisation twice. In order to be consistent, both datasets shown in Fig. 2 include this contribution due to symmetric dissociative ionisation (which is, however, small, see [5,7]) twice. All calculated cross sections, on the other hand, count this contribution only once. The level of agreement between the various datasets is reasonably good. All calculated curves, which are in very good agreement among each other, lie slightly above the data of [7] and are closer to the data of [18], which, on the other hand, carry a large margin of uncertainty due to the error bars of the original data of Van Zyl and Dunn [22].

In the case of O_2^+ (Fig. 3), we compare the calculated DM cross section with recently measured [23] cross sections for the ionisation and dissociative ionisation of O_2^+, which is the dominant ionisation channel, but which has a cross section that is considerably smaller than the cross section for dissociative excitation. The calculated cross section exceeds the combined measured cross sections for ionisation and dissociative ionisation by about a factor of 2. There are no other calculated cross section data available for this ion.

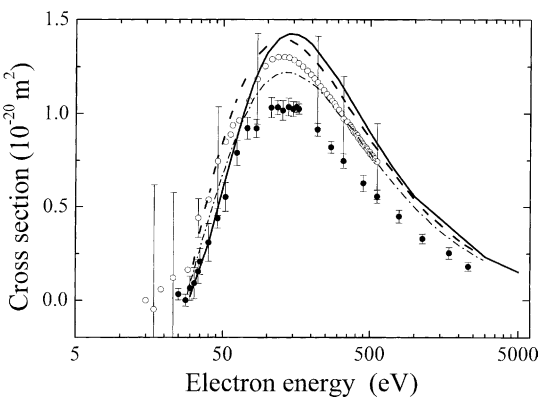

Fig. 2. Calculated DM cross section for the electron-impact ionization of N_2^+ (thick solid curve) as a function of electron energy in comparison with various measured and other calculated cross sections. The experimental datasets are those of [8] (filled circles) and [21] (open circles). The dot-dashed line and the dashed line refer to two variants of the BEB calculation [5] using two different wave functions for the ground-state ion.

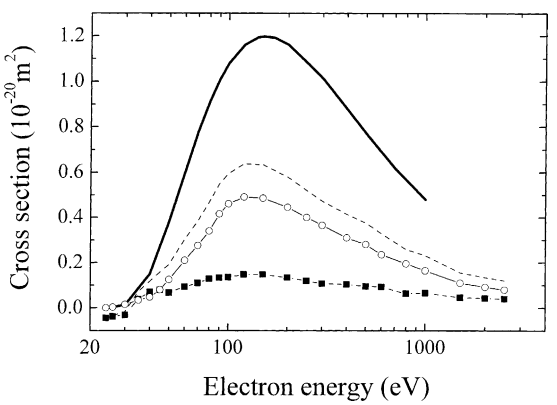

Fig. 3. Calculated DM cross section for the electron impact ionization of O_2^+ (thick solid line) as a function of electron energy in comparison with the measured partial cross sections for ionization (filled squares) and dissociative ionization (circles) of O_2^+ [23]. Also show is the sum of the two partial cross sections (dashed line).

3.2. The heteronuclear diatomic ions CD^+ and CO^+

Djuric et al. [24] measured the cross section for the production of D^+ following electron impact on CD^+ which includes contributions from both the dissociative excitation and the dissociative ionisation of the target ion. These authors also provide an estimate for the fraction of their measured cross section that is attributable to dissociative ionisation, i.e., the formation of $D^+ + C^+$. This curve is shown in Fig. 4 in comparison with a calculated BED cross section [5] and our DM cross section. The BED cross section agrees well with the extracted cross section for the dissociative ionisation of CD^+, whereas the DM cross section exceeds both the experimentally determined data and the BED cross section by about 40%. It must be noted, however, that the total CD^+ ionisation cross section, which we calculate, also includes a contribution for the ionisation of the parent CD^+ ion (i.e., formation of CD^{2+}) and for the dissociative ionisation leading to the formation of C^{2+} ions. This may well explain the discrepancy between the DM cross section and the experimental data shown in Fig. 4. No experimental data are available in the literature for the ionisation cross section of the parent CD^+ ion or for the dissociative ionisation leading to C^{2+}.

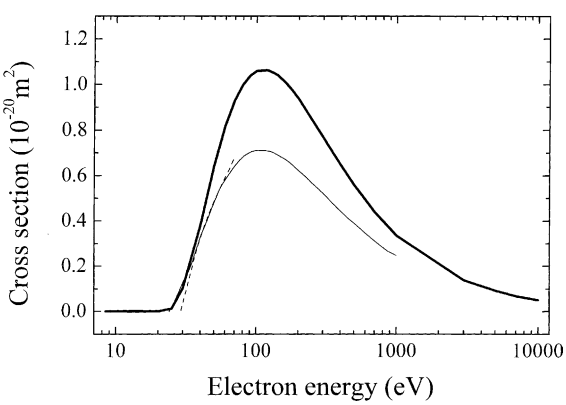

Fig. 4. Calculated DM cross section for the electron impact ionization of CD^+ (thick solid line) as a function of electron energy in comparison with the calculated BEB cross section [5] (thin solid line) and the measured partial cross section for dissociative ionization of CD^+ leading to the formation of D^+ ions [24] (dashed line).

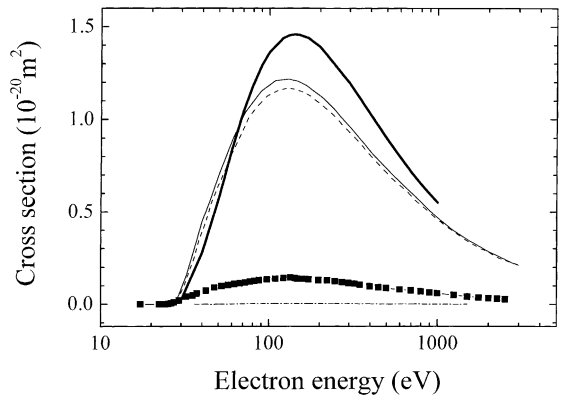

Fig. 5. Calculated DM cross section for the electron impact ionization of CO^+ (thick solid line) as a function of electron energy in comparison with two calculated cross sections using the BEB method [5] (thin solid line and dashed line) and the measured cross sections for the ionization of CO^+ (filled squares) and the sum of the two partial cross sections for dissociative ionization of CO^+ leading to the formation of respectively C^{2+} and O^{2+} ions [25] (dash-dot line).

Fig. 5 shows the calculated DM cross section for the ionisation of CO^+ in comparison with two variants of the calculated BEB cross section [5] and with experimental data obtained by Defrance and co-workers [25]. The two experimental datasets shown in Fig. 5 refer to the partial cross sections for ionisation of CO^+ leading to the formation of CO ions and to the sum of the cross sections for the dissociative ionisation leading to the formation of C^{2+} ions and O^{2+} ions, respectively. The three calculated cross sections agree with each other to within 20%, but exceed the sum of measured partial ionisation cross sections by almost a factor of 10. One possible explanation for this significant discrepancy may be the fact that the doubly charged CO^{2+} ion is highly unstable because two bonding electrons are missing compared to the neutral CO molecule. As a consequence, a significant fraction of these doubly charged ions may undergo fragmentation before they reach the detector and thus remain undetected in the experiment. To the best of our knowledge, nothing is known from experimental

studies regarding the dissociative ionisation of CO^+ leading to the formation of $C^+ + O^+$.

3.3. The polyatomic ions CO_2^+, H_3O^+/D_3O^+, and CD_4^+

The molecular ion CO_2^+ was already discussed in our earlier letter [6]. However, some conclusions relating to the summation of the measured partial cross sections that were discussed in the previous publication [6] need to be revised as discussed below. Fig. 6 shows the measured CO_2^{2+}, C^+, and O^+ partial ionisation cross sections [7,8] together with their sum (labelled as "Σ") in comparison with the DM calculation for the single ionisation of CO_2^+. The measured as well as the calculated data show a broad peak around 100 eV and a similar energy dependence. However, the maximum value of the calculated cross section of about 2×10^{-16} cm^2 exceeds the measured peak value of about 1.2×10^{-16} cm^2 by almost a factor of 2. Previously, we added maximum values of unpublished cross sections [26] for the formation of CO^+ and O_2^+ to the maximum of the sum of the CO_2^+, C^+, and O^+ partial cross sections to obtain a corrected cross section "Σ_{corr}" with a maximum value of about 1.8×10^{-16} cm^2. However, these two contributions are already included in the measured C^+ and O^+ cross sections and were thus counted twice. The cross section labelled "Σ_{corr}" that was included in Fig. 1 in [6] has been omitted in Fig. 6 shown here.

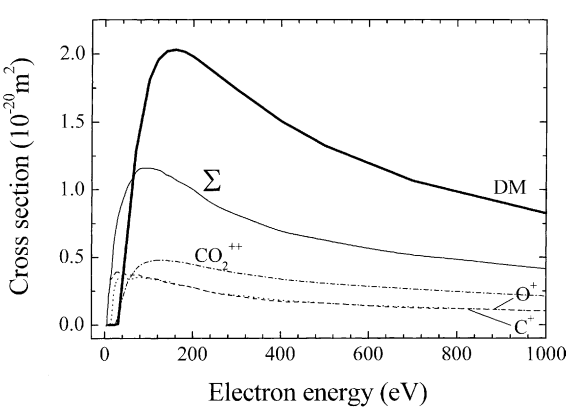

Fig. 6. Calculated DM cross section for the electron impact ionization of CO_2^+ (thick solid line) as a function of electron energy in comparison with various measured partial ionization cross sections [7]. The various curves are labelled in the diagram and further details are given in the text.

For both H_3O^+/D_3O^+ and CD_4^+ the direct ionisation cross sections leading to the formation of the doubly charged parent ions are generally small compared to the dissociative ionisation cross sections. In both cases, partial cross sections have been measured by several authors [27–29] for the formation of various particular fragment ions; in the case of H_3O^+/D_3O^+, all fragmentation studies were carried out using the deuterated target. All measured cross sections relating to fragmentation channels contain contributions from the dissociative excitation as well as the dissociative ionisation. No attempt was made by the authors of [28,29] to separate the two contributions. However, since only the contribution attributable to dissociative ionisation can be included in the comparison between experimental and the calculated ionisation cross sections, it is necessary to extract this contribution from the reported datasets. This is not always easy and straightforward (see below).

Fig. 7 shows the calculated DM cross section for the ionisation of H_3O^+ in comparison with measured

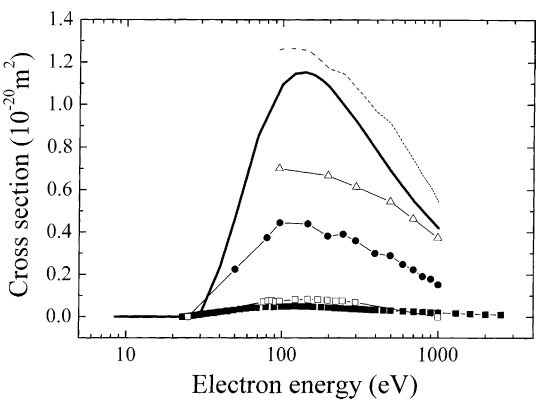

Fig. 7. Calculated DM cross section for the electron impact ionization of H_3O^+ (thick solid line) as a function of electron energy in comparison with the measured partial cross sections [27,28]. The various datasets refer to the ionization of H_3O^+ (filled squares) and the dissociative ionization leading to OH (filled circles) and O^+ (open squares). Also shown are the data for formation of H_2O^+ (open triangles) from [28] above 100 eV (see text for details) and the sum of all partial cross sections (dashed line).

data from Bahati et al. [27] and Schulz et al. [28] obtained for H_3O^+ as well as for D_3O^+ as the target. The measured data shown in Fig. 7 are the cross sections for ionisation of H_3O^+ from [27] and the cross sections for dissociative ionisation of H_3O^+ leading to the formation of O^+ and OH^+ from [28]. In the latter two cases the contributions attributable to the dissociative ionisation have been extracted from the reported dataset, which include contributions from dissociative excitation and dissociative ionisation using estimated cross section shapes for the respective contributions in conjunction with the known threshold for dissociative ionisation. Also shown in Fig. 7 is the cross section for the formation of D_2O^+ from D_3O^+ from [28] which also contains contributions from both dissociative excitation and dissociative ionisation. In this case, too few data points were reported in [28] to allow a meaningful extraction of the fraction of the cross section attributable to dissociative ionisation. Therefore, we show in Fig. 7 the data for the formation of D_2O^+ as reported in [28], but limit the data to impact energies above about 100 eV where dissociative ionisation is expected to be the more important process. The lack of data for the formation of D_2O^+ ions is unfortunate as this process appears to have the largest partial ionisation cross section and a more reliable way of extracting data for the dissociative ionisation leading to the formation of this ion would be desirable. We also show in Fig. 7 the sum of all experimentally determined partial ionisation cross sections for energies above 100 eV. This sum cross section, which should be considered an upper limit because of a possible residual contribution due to dissociative excitation in the extracted D_2O^+ partial cross section, is in reasonably good agreement with the calculated DM cross section. No data are available for the dissociative ionisation of H_3O^+ leading to the formation of O^{2+} fragment ions, which is a process whose cross section is expected to be small (see discussion before).

Fig. 8 shows the calculated DM cross section for the ionisation of CD_4^+ in comparison with available experimental data which are unpublished [29]. In addition to the parent ionisation cross section (CD_4^{2+} formation), which is very small, we show dissociative ionisation cross sections for the formation of CD_3^+, CD_2^+, CD^+, and C^+ fragment ions. For all fragment ions, the datasets shown in Fig. 8 represent estimates for the fraction of the measured partial cross section that is attributable to dissociative ionisation and these fractions have been extracted from the measured data which also include contributions from the dissociative excitation using a procedure similar to the one described above in the case of H_3O^+. We note, however, that the fraction of the cross section for formation of CD_3^+ ions attributable to dissociative ionisation is impossible to extract in a meaningful fashion, since the authors of [29] report only six data points in the low-energy regime from about 8–45 eV. For reasons of completeness, we include a single CD_3^+ data point at the highest impact energy of 45 eV for which data are reported in [28]. This cross section includes contributions from both dissociative excitation and dissociative ionisation. It is unfortunate that the CD_3^+ dataset is too limited to extract a meaningful dissociative ionisation cross section for the formation of the CD_3^+ fragment ion, which appears to be very important channel. Also shown in Fig. 8 is the sum of all partial cross

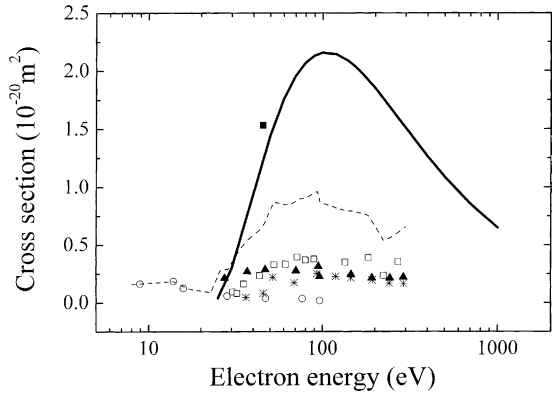

Fig. 8. Calculated DM cross section for the electron impact ionization of CD_4^+ (thick solid line) as a function of electron energy in comparison with the measured partial cross sections [29]. The various datasets refer to the ionization of CD_4^+ (open circles) and the dissociative ionization leading to CD_2^+ (filled triangles), CD^+ (open squares), and C^+ (stars). A single data point (filled square) is given for the formation of CD_3^+ fragment ions (see text for details). Also shown is the sum of all partial cross sections exclusive of the CD_3^+ data point (dashed line).

sections exclusive of any contribution from the CD_3^+ channel. The scatter in the data points of this cross section as a function of impact energy reflects the fact that the various reported partial cross sections carry large uncertainties that render a meaningful extraction of dissociative ionisation cross sections difficult. The calculated DM cross section exceeds the experimental cross section by more than a factor of 2 in terms of the maximum cross section value. Clearly, the inclusion of the dissociative ionisation channel leading to the formation of CD_3^+ ions will improve the agreement between experiment and calculation.

4. Conclusions

We used the semi-classical Deutsch–Märk (DM) formalism to calculate absolute electron-impact ionisation cross section of the molecular ions H_2^+, N_2^+, O_2^+, CD^+, CO^+, CO_2^+, H_3O^+/D_3O^+, and CD_4^+ for which experimental data have been reported. In many cases it is difficult to extract meaningful and reliable partial cross sections for the formation of a particular fragment ion that is attributable to dissociative ionisation from measured data that include contributions from both dissociative excitation and dissociative ionisation. The level of agreement between the experimentally determined and the calculated cross section is satisfactory only in a few cases. In other cases, there are significant discrepancies of up to a factor 2 and up to almost a factor 10 for CO^+. In most cases, the calculated cross sections exceed the measured cross sections which is not surprising in view of the experimental complications in measuring reliable ionisation cross sections for molecular ions due to the presence of competing channels for the formation of fragment ions.

Acknowledgements

This work has been carried out within the Association EURATOM-ÖAW. The content of the publication is the sole responsibility of its publishers and it does not necessarily represent the views of the EU Commission or its services. It was partially supported by the FWF, ÖNB, and ÖAW, Wien, Austria. One of us (K.B.) acknowledges partial financial support from the U.S. National Aeronautics and Space Administration (NASA) under grant NAG5-8971.

References

[1] H. Deutsch, K. Becker, S. Matt, T.D. Märk, Int. J. Mass Spectrom. 197 (2000) 37.
[2] M. Probst, H. Deutsch, K. Becker, T.D. Märk, Int. J. Mass Spectrom. Ion Process. 206 (2001) 13.
[3] Y.-K. Kim, M.E. Rudd, Phys. Rev. A 50 (1994) 3954.
[4] W. Hwang, Y.-K. Kim, M.E. Rudd, J. Chem. Phys. 104 (1996) 2956.
[5] Y.K. Kim, K.K. Irikura, M.A. Ali, J. Res. NIST 105 (2000) 285.
[6] H. Deutsch, K. Becker, P. Defrance, U. Onthong, R. Parajuli, M. Probst, S. Matt, T.D. Märk, J. Phys. B 35 (2002) L65.
[7] E.M. Bahati, J.J. Jureta, D.S. Belic, S. Rachafi, P. Defrance, J. Phys. B 34 (2001) 1757.
[8] E.M. Bahati, J.J. Jureta, D.S. Belic, H. Cherkani-Hassani, M.O. Abdellahi, P. Defrance, J. Phys. B 34 (2001) 2963.
[9] H. Deutsch, T.D. Märk, Int. J. Mass Spectrom. Ion Process. 79 (1987) R1.
[10] J.P. Desclaux, Atom. Data Nucl. Data Tables 12 (1973) 325.
[11] R.S. Mullikan, J. Chem. Phys. 23 (1955) 1833.
[12] R. Tang, J. Callaway, J. Chem. Phys. 84 (1986) 6858.
[13] W. Stevens, H. Basch, J. Krauss, J. Chem. Phys. 81 (1984) 6026.
[14] W. von Nissen, J. Schirmer, L.S. Cederbaum, Comp. Phys. Rep. 1 (1984) 57.
[15] H.C. Straub, B.G. Lindsay, K.A. Smith, R.F. Stebbings, J. Chem. Phys. 105 (1996) 4015.
[16] C. Tian, C.R. Vidal, J. Chem. Phys. 108 (1997) 927.
[17] C. Tian, C.R. Vidal, Phys. Rev. A 58 (1998) 3783.
[18] B. Peart, K.T. Dolder, J. Phys. B 6 (1973) 2409.
[19] K.C. Mathur, A.N. Tripathi, S.K. Joshi, Phys. Rev. A 1 (1970) 1404.
[20] R.G. Aismiller Jr., Oak Ridge National Laboratory Report ORNL-2766, 1962, unpublished.
[21] J.R. Peterson, et al., J. Chem. Phys. 108 (1998) 1978.
[22] B. Van Zyl, G.H. Dunn, Phys. Rev. 163 (1967) 43.
[23] P. Defrance, private communication, 2002 and to be published.
[24] N. Djuric, Y.-S. Chung, B. Wallbank, G.H. Dunn, Phys. Rev. A 56 (1997) 2887.
[25] D.S. Belic, D.J. Yu, A. Sharif, P. Defrance, J. Phys. B 30 (1997) 5535.
[26] P. Defrance, private communication, 2001 and to be published.
[27] E.M. Bahati, J.J. Jureta, H. Cherkani-Hassani, P. Defrance, J. Phys. B 34 (2001) L1.
[28] P.A. Schulz, D.C. Gregory, F. Meyer, R.A. Phaneuf, J. Chem. Phys. 85 (1986) 3386.
[29] D.C. Greory et al., Oak Ridge National Laboratory Internal Report, ORNL-DWG-92, 1989.